JOURNAL OF CHEMICAL INFORMATION AND MODELING

ARTICLE

pubs.acs.org/jcim

Inhibitor and Substrate Binding by Angiotensin-Converting Enzyme: Quantum Mechanical/Molecular Mechanical Molecular Dynamics Studies

Xuemei Wang,[†] Shanshan Wu,[†] Dingguo Xu,[*,†] Daiqian Xie,[‡] and Hua Guo[§]

[†]Key Laboratory of Green Chemistry & Technology, Ministry of Education, College of Chemistry, Sichuan University, Chengdu, Sichuan 610064, China

[‡]Institute of Theoretical and Computational Chemistry, Key Laboratory of Mesoscopic Chemistry, School of Chemistry and Chemical Engineering, Nanjing University, Nanjing 210093, China

[§]Department of Chemistry and Chemical Biology, University of New Mexico, Albuquerque, New Mexico 87131, United States

ABSTRACT: Angiotensin-converting enzyme (ACE) is an important zinc-dependent hydrolase responsible for converting the inactive angiotensin I to the vasoconstrictor angiotensin II and for inactivating the vasodilator bradykinin. However, the substrate binding mode of ACE has not been completely understood. In this work, we propose a model for an ACE Michaelis complex based on two known X-ray structures of inhibitor-enzyme complexes. Specifically, the human testis angiotensin-converting enzyme (tACE) complexed with two clinic drugs were first investigated using a combined quantum mechanical and molecular mechanical (QM/MM) approach. The structural parameters obtained from the 550 ps molecular dynamics simulations are in excellent agreement with the X-ray structures, validating the QM/MM approach. Based on these structures, a model for the Michaelis complex was proposed and simulated using the same computational protocol. Implications to ACE catalysis are discussed.

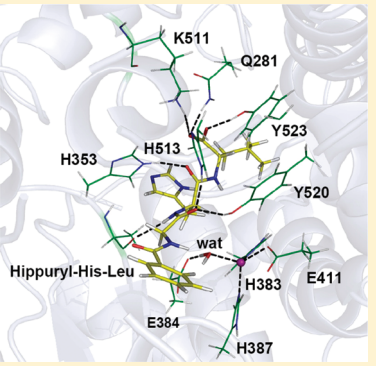

1. INTRODUCTION

The angiotensin-converting enzyme (ACE) is a zinc-dependent dipeptidase, which was discovered more than half a century ago.[1] This enzyme exhibits an important biological function in regulating the conversion of the biologically inactive angiotensin I to angiotensin II, a powerful vasoconstrictor. It is also involved in the inactivation of bradykinin, a potent vasodilator. The dual functionality is now known to play a key role in the blood pressure regulating renin-angiotensin system (RAS). As a result, ACE is a prominent target for treating hypertension and cardiovascular diseases.[2,3] Although several FDA approved ACE inhibitors are already available for clinic use, the substrate binding and catalysis of ACE are still not completely understood. Interestingly, the first few ACE inhibitors were identified using carboxypeptidase A (CPA) or thermolysin (TLN) as a model,[4,5] which was believed to have a similar active-site architecture. It is only recently that the three-dimensional structure of ACE was determined via X-ray diffraction.[6] While confirming the similarities of the active sites among these enzymes, ACE was shown to have a vastly different overall fold from CPA and TLN.

Two types of ACE are known. The human somatic angiotensin-converting enzyme (sACE) has two domains, namely the N domain and the C domain. They have about 55% sequence similarity,[7] but both domains contain the same zinc binding motif, HEXXH, and a downstream E residue.[8] This phenomenon is thought to be a result of gene duplication. The C domain was found to be the dominant angiotensin-converting site in controlling blood pressure and cardiovascular functions, based on the observation that the inhibition of the N domain has little effect on these functions.[9] Another form of ACE is found in testis, which plays a role in fertilization. The testicular ACE (tACE) shows an identical active site with the C domain of sACE but has no N domain.[10] Recently, three-dimensional structures of various ACEs have been determined.[6,11−16]

An interesting structural characteristic of ACE is the presence of two chloride ions outside the active site. Experiments indicated that they are essential to maintain the binding structure and catalytic activity.[17−19] Based on X-ray structures of ACE, the Cl^- ion at the first binding position (I) is about 21 Å away from the zinc ion. It is in hydrogen bonding distances with Arg186 and Arg489 and exhibits van der Waals interactions with a shell formed by Trp485, Trp486 side chain groups and the Asp507 backbone. These interactions are thought to be very important for the stabilization of the enzyme−substrate complex.[20] The chloride ion at the second binding position (II) is about 10 Å away from the zinc ion and is in hydrogen bonding distances with Arg522, Tyr224, and a water. In addition, a hydrophobic shell formed by residues of Pro407, Pro519, and Ile521 was found to surround Cl^-(II). Kinetic experiments suggested that Cl^-(II) is critical for enzyme catalysis.[17,19] In our simulations, both anions

Received: February 16, 2011
Published: April 26, 2011

are included in the model, but this work will not focus on the roles played by these two important anions.

The search for effective ACE inhibitors has a long history.[3,21,22] It is remarkable that the first inhibitor (captopril) was discovered serendipitously using CPA as a model,[23] without the structure of ACE. Subsequently, other potent inhibitors of ACE were reported,[5,24−26] again without knowledge of its structure. Very recently, several ACE structures in complex with inhibitors have been reported, as shown in Table 1 along with the corresponding inhibition constants. The availability of ACE structures opened the door for the rational design of new and improved ACE inhibitors.[27,28] The early stage inhibitors of ACE had less specificity to the C or N domains, thus exhibiting adverse side effects. More recently, there is a keen interest in developing new inhibitors with high specificity to one of two domains.[27,29] Some success, e.g., RXP407 to the N domain[25] and RXPA380 to the C domain,[26] have been reported. The emergence of domain-selective inhibitors calls for more studies of the substrate or inhibitor binding mode to different domains, as a recent study showed that the basis of domain-dependent inhibition of ACEs might come from interactions between bulky hydrophobic side chain moieties and the domain-specific hydrophobic residues.[15]

The widespread use of ACE inhibitors in clinic settings underscores the importance for understanding the binding and catalytic modes of the enzyme at the microscopic level. Experimental studies alone are often insufficient to answer all questions and computational models can offer a complementary perspective. Despite the rapid accumulation of structural and kinetic data, however, there have been few computational studies on this important system. An earlier density functional theory study focused on a truncated active-site model,[30] while more recent ones investigated docking of various small molecule inhibitors to ACE.[31,32] These studies provided no dynamical information concerning the fluctuation of the enzymatic system. A recent molecular dynamics study on an enzyme−substrate complex has been reported by Papakyriakou et al.,[33] using a modified Amber force field. To avoid the well-known problems associated with a force-field description of the zinc-ligand bonds as electrostatic interactions,[34,35] a bonded approach[36] was used in which an artificial force field for the zinc-ligand interactions was determined based on *ab initio* calculations.

In this work, we attempt to establish the structure of the Michaelis complex for ACE using a quantum mechanical/molecular mechanical approach. Our simulations are based on the known structures of ACE in complex with two inhibitors: enalaprilat and lisinopril.[6,11] These two inhibitors are effective ACE inhibitors that have been extensively used in blood-pressure control therapy.[22] The backbones of these inhibitors are very close to a natural substrate of ACE, Hip-His-Leu, as shown in Scheme 1. Such a structural similarity allowed us to propose a plausible substrate binding mode based on the simulation of inhibitor-enzyme complexes. We further constrain our model to conform with several known determinants in CPA and TLN catalysis concerned with the interaction with the zinc cofactor.

2. METHOD AND PROTOCOL

2A. Quantum Mechanical/Molecular Mechanical Method. The computational approach used to describe the active-site dynamics is a combined quantum mechanical and molecular mechanical (QM/MM) method,[37−39] which divides the system into two parts. A smaller QM region consists of those residues related to reaction, while the surrounding MM region contains most of the environment residues and solvent. The MM region is represented by the all-atom CHARMM force field[40] and TIP3P water.[41] The QM-MM boundary is treated with the link-atom method.[38] The selection of the method to treat the QM region is critical for the computational efficiency and accuracy. In this work, we will use the self-consistent charge-density functional tight binding (SCC-DFTB) method[42−44] to perform the electronic structure calculations for the QM region. The SCC-DFTB parameters for the biological zinc ion have been developed,[45] and the SCC-DFTB/CHARMM approach has been successfully validated in several zinc enzymes, including carbonic anhydrase,[46,47] carboxypeptidase A,[48,49] and metallo-β-lactamases.[50−55] Since ACE has a similar active-site construct, this QM/MM scheme should be able to characterize the enzyme well.

Table 1. List of X-ray Structures of tACE Complexed with Various Inhibitors

PDB code	inhibitors	K_i (μM)	ref
2OC2	RXPA380	0.003[a]	14
1O86	lisinopril	0.00027[b]	6
1UZF	captopril	0.00111[b]	11
1UZE	enalaprilat	0.00078[b]	11
3BKK	kAF	0.83[a]	15
3BKL	kAW	0.679[a]	15

[a] 200 mM Cl^-. [b] 20 mM Cl^-.

Scheme 1. Structural Comparison of Hip-His-Leu, Lisinopril, and Enalaprilat, Where the Zn^{2+} Binding Is Indicated by Red Asterisks

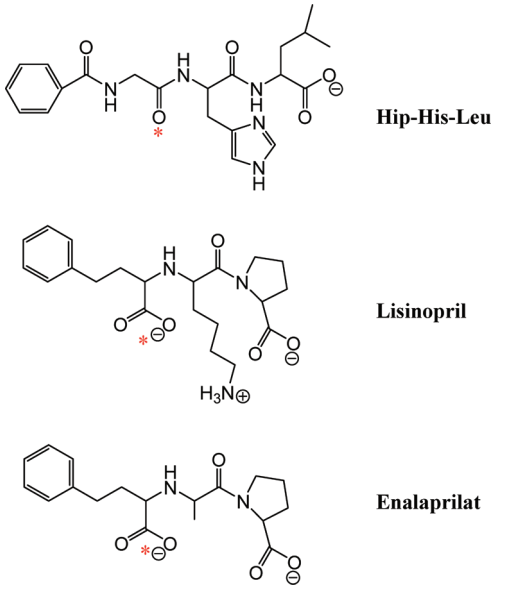

2B. Enzyme−Inhibitor Complex Models. The initial structures for two enzyme−inhibitor complexes were obtained from the Protein Data Bank (PDB codes: 1O86[6] and 1UZE[11]). For both models, the sole zinc ion is bound with the side chains of His383, His387, and Glu411. The fourth ligand of the zinc ion is provided by the carboxylate group of the inhibitors. In our models, the disulfide bonds between Cys152 and Cys158,

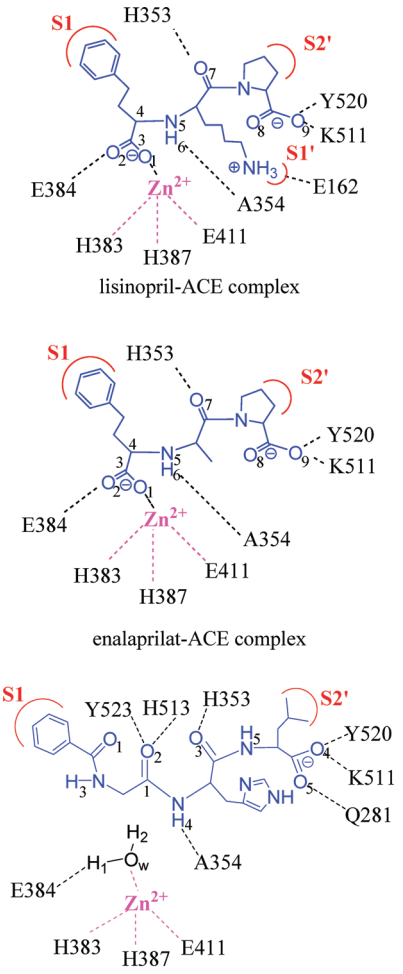

Figure 1. Atom definition and corresponding interactions between inhibitors/substrate and active-site residues of tACE.

Cys352 and Cys370, and between Cys538 and Cys550 were enforced. The HBUILD module of CHARMM was used to assign hydrogen atoms to residues. Special attention was paid for the ionization states of key titratable groups. For example, Glu384 in the active site was assigned to be protonated, judging by the distance between its carboxylate oxygen and the inhibitor carboxylate group as shown in Figure 1. In addition, the side chain of the lysine residue of the lisinopril molecule was treated in the ionized form since the X-ray structure was obtained at pH = 4.7.[6]

The systems were then solvated with a pre-equilibrated TIP3P water[41] sphere of a 25 Å radius centered at the zinc ion, followed by 30 ps molecular dynamics (MD) simulation with all of enzyme residues, inhibitors, zinc, and Cl^- ions fixed. This process was performed several times with randomly rotated water spheres to ensure uniformly solvation. Subsequently, stochastic boundary conditions[56] were applied to reduce the computational costs. In particular, those atoms that are 25 Å away from the origin were removed, while atoms in the buffer zone (22 Å < r < 25 Å) were subjected to Langevin dynamics with friction and random forces. In the inner reaction zone (r < 22 Å), the atoms follow Newtonian dynamics on the hybrid QM/MM potential energy hypersurface. A group-based switching scheme was used for nonbonded interactions.[57]

In this work, the QM region includes the metal ion, the inhibitor molecule, and the side chain groups of His383, His387, Glu411, and Glu384 residues. The labeling of active-site atoms is provided in Figure 1. Since the Cl^- ions are outside the active site, they were simulated in the MM region. For both models, a total 550 ps MD simulation was performed with an integration time step of 1.0 fs. The temperature was slowly heated to 300 K in 30 ps, and another 70 ps MD was allowed for further equilibration. The subsequent 450 ps MD trajectory was used for the data analysis. The SHAKE algorithm[58] was applied to restrain the covalent bonds involving hydrogen atoms.

2C. Michaelis Complex. The MD simulations of the enzyme−inhibitor complexes provide a good starting point to postulate the binding mode for a *bona fide* substrate of ACE. In this work, a natural substrate molecule, hippuryl-L-histidyl-L-leucine (Hip-His-Leu),[59] was employed in the simulation of the Michaelis complex. Our binding model differs significantly from the suggestion made by Sturrock et al.,[7] with a tripeptide molecule, Phe-His-Leu. In their model, the fourth ligand of the zinc ion was postulated to be the carbonyl oxygen of the scissile bond in the substrate, and a nonzinc bound water molecule is present in the active site with a hydrogen bond with Glu384. However, such an arrangement is at odds with that in the active sites of the extensively studied CPA and TLN, which are believed to have the same catalytic mechanism as ACE. In an earlier study on TLN, Hangauer et al. suggested that the fourth ligand of the zinc ion is a water molecule which serves as the nucleophile when activated by a general base (Glu143).[60] Such a mechanism has recently been confirmed computationally by Blumberger et al.[61] A similar binding model and mechanism were proposed for CPA[62] and recently verified with a QM/MM model.[48]

Our model of the Michaelis complex is based on the premise that the fundamental binding determinants of ACE should be similar to TLN and CPA. In other words, the fourth ligand of the zinc ion is the water nucleophile hydrogen bonded with the general base (Glu384) and the backbone carbonyl oxygen only interacts weakly with the metal ion. This model is reasonable, given the small (0.52 Å) rmsd between the active sites of ACE and TLN.[6] It is believed that the ligand-free ACE has a water molecule bound to the zinc ion as its fourth ligand.[6] Since the metal binding site of both inhibitors (labeled by red asterisks in Scheme 1) consists of a negatively charged carboxylate group, it is not difficult to image the water to be displaced by the anionic group which is known to interact strongly with the zinc ion. On the other hand, the carboxylate group is replaced by a neutral carbonyl oxygen in the substrate, which generally does not interact strongly with the zinc ion.[15] Thus, when the substrate enters the binding site, it is unlikely to dislodge the zinc-bound water, as in the case of CPA and TLN.

The corresponding atom definitions and interactions between the substrate and active-site residues are given in Figure 1. To build the model for the Michaelis complex, we first removed the lisinopril molecular from the active site of tACE (PDB code 1O86).[6] The Hip-His-Leu substrate was then manually docked in the active site in the appropriate orientation. This approach is similar to the work of Papakyriakou et al.[33] but with a QM/MM description of the system. The subsequent setup protocol is essentially the same as that for the enzyme−inhibitor models. Specifically, the QM system includes the zinc ion, side chain groups of its three protein ligands, the entire substrate, the water nucleophile, and the deprotonated carboxylate of the general base (Glu384). A total of one nanosecond MD simulation was

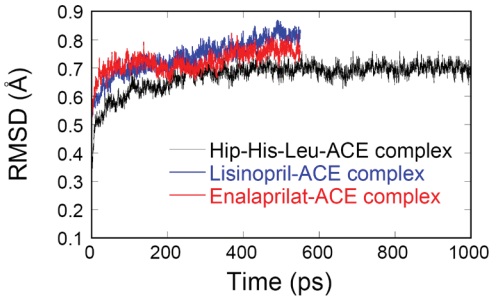

Figure 2. RMSDs for both enzyme−inhibitor complexes and enzyme−substrate complex as a function of time.

Table 2. Key Geometric Parameters at the Active Site of the Lisinopril-ACE Complex

bond length (Å) and bond angle (deg)	QM/MM MD	X-ray[6]
$Zn\cdots N_{\varepsilon 2}$ (H383)	2.02 ± 0.06	2.04
$Zn\cdots N_{\varepsilon 2}$ (H387)	1.98 ± 0.06	2.07
$Zn\cdots O_{\varepsilon 1}$ (E411)	2.06 ± 0.07	1.99
$Zn\cdots O_1$	2.09 ± 0.14	2.14
$O_2\cdots H_{\varepsilon 2}$(E384)	1.78 ± 0.15	2.69
$O_9\cdots H_{\zeta 1}$(K511)	1.59 ± 0.09	2.93[a]
$O_9\cdots H_{\eta}$(Y520)	1.70 ± 0.13	2.55[b]
$O_7\cdots H_{\varepsilon 2}$(H353)	1.97 ± 0.25	2.76[a]
$O_1\cdots H_{\eta}$(Y523)	1.86 ± 0.24	2.77[b]
$H_6\cdots$O(A354)	2.36 ± 0.59	2.92
$O_{\varepsilon 2}$(E162)$\cdots H_{\zeta}$(Lys)	1.81 ± 0.30[e]	3.45
Cl···Zn	10.14 ± 0.29	10.37
$Cl\cdots H_{\varepsilon}$(R522)	1.95 ± 0.14	3.08[c]
$Cl\cdots H_{22}$(R522)	1.93 ± 0.15	3.55[c]
$Cl\cdots H_{\eta}$(Y224)	1.85 ± 0.35	3.01[d]
$N_{\varepsilon 2}$(H383)$\cdots$Zn$\cdots O_1$	110.4 ± 8.1	116.8
$N_{\varepsilon 2}$(H387)$\cdots$Zn$\cdots O_1$	125.2 ± 7.8	123.0
$O_{\varepsilon 1}$(E411)$\cdots$Zn$\cdots O_1$	104.2 ± 8.3	98.8

[a] Distance between O and O atoms. [b] Distance between O and N atoms. [c] Distance between Cl and N atoms. [d] Distance between Cl and O atoms. [e] Averaged distance between $O_{\varepsilon 2}$ and the H_{ζ} involved in hydrogen bonding.

carried out for the substrate-enzyme complex. The first 300 ps were used to sufficiently relax the whole system, while the subsequent trajectory of 700 ps was employed for data analysis.

3. RESULTS

3A. Dynamics Enzyme−Inhibitor Complexes. *Active Site Binding Pattern.* The binding modes for the two inhibitors based on the X-ray structures are displayed in Figure 1. Both enalaprilat and lisinopril are bound with the enzyme through a direct contact with the metal ion via the C_4-carboxylate group. The so-called carboxylate class of ACE inhibitors differs from the sulfhydryls such as captopril, which binds the enzyme via its sulfide as the fourth ligand of the zinc ion.[29] No other covalent bonds between inhibitors and enzyme residues are present in the crystal structures or in our models.

To understand the detailed dynamic features of the inhibitor binding, we performed QM/MM MD simulations for two enzyme−inhibitor complexes. Both structures are quite stable

Table 3. Key Geometric Parameters at the Active Site in the Enalaprilat-ACE Complex

bond length (Å) and bond angle (deg)	QM/MM MD	X-ray[11]
$Zn\cdots N_{\varepsilon 2}$(H383)	1.99 ± 0.06	2.10
$Zn\cdots N_{\varepsilon 2}$(H387)	1.98 ± 0.06	2.05
$Zn\cdots O_{\varepsilon 1}$(E411)	2.04 ± 0.07	1.89
$Zn\cdots O_1$	2.08 ± 0.08	2.01
$O_2\cdots H_{\varepsilon 2}$(E384)	1.82 ± 0.16	2.71[a]
$O_9\cdots H_{\zeta 1}$(K511)	1.65 ± 0.14	2.84[b]
$O_9\cdots H_{\eta}$(Y520)	1.71 ± 0.20	2.61[a]
$O_7\cdots H_{\varepsilon 2}$(H353)	1.95 ± 0.25	2.68[b]
$O_1\cdots H_{\eta}$(Y523)	1.72 ± 0.14	2.82[a]
$H_6\cdots$O(A354)	1.94 ± 0.24	2.96[b]
Cl···Zn	10.11 ± 0.31	10.40
$Cl\cdots H_{\varepsilon}$(R522)	1.89 ± 0.12	3.15[c]
$Cl\cdots H_{22}$(R522)	1.96 ± 0.16	3.53[c]
$Cl\cdots H_{\eta}$(Y224)	1.85 ± 0.31	3.09[d]
$N_{\varepsilon 2}$(H383)$\cdots$Zn$\cdots O_1$	110.7 ± 7.6	116.5
$N_{\varepsilon 2}$(H387)$\cdots$Zn$\cdots O_1$	118.9 ± 7.8	125.2
$O_{\varepsilon 1}$(E411)$\cdots$Zn$\cdots O_1$	103.5 ± 7.3	103.6

[a] Distance between O−O atoms. [b] Distance between O−N atoms. [c] Distance between Cl and N atoms. [d] Distance between Cl and O atoms.

during the MD simulations. As Figure 2 shows, the root-mean-square deviations (RMSDs) for the backbone atoms are 0.77 ± 0.06 Å for the lisinopril-ACE complex and 0.76 ± 0.04 Å for the enalaprilat-ACE complex, respectively. Selected internuclear distances averaged over the trajectories are listed in Tables 2 and 3, and two snapshots for the inhibitor-enzyme complex are displayed in Figure 3.

In agreement with the crystal structures, the tetra-coordination for the zinc ion was maintained for both inhibitors throughout our simulations. The zinc ligands consist of His383, His387, Glu411, and the C_4 carboxylate oxygen (O_1) of lisinopril or enalaprilat. The O_1−Zn distance is 2.09 ± 0.14 Å and 2.08 ± 0.08 Å for lisinopril and enalaprilat, respectively, which can be compared with the X-ray values of 2.14 Å and 2.01 Å. As discussed below, O_1 is also hydrogen bonded with the side chain of Try523.

For the two inhibitors studied in this work, the binding patterns are quite similar. As shown in Figures 1 and 3, the lysine residue of lisinopril interacts strongly with the Glu162 residue at the S1′ subsite of the enzyme, although the three hydrogen atoms of the lysine switch their positions during the MD simulation. On the other hand, the methyl group of enalaprilat makes no such contact, which could be the reason why lisinopril has a stronger binding affinity than enalaprilat. At the S1 site, the phenyl group of the inhibitors is surrounded by two hydrophobic residues, Phe512 and Val518, and two water molecules. On the other hand, the C-terminal proline residue of the inhibitor is stabilized in the S2′ subsite of ACE by hydrogen bonds to its carboxylate oxygens. In particular, O_9 of the proline terminal carboxylate group is hydrogen bonded with Lys511 and Tyr520, with the hydrogen bond distances of 1.59 ± 0.09 Å and 1.70 ± 0.13 Å in lisinopril, 1.65 ± 0.14 Å and 1.71 ± 0.20 Å in enalaprilat. The other carboxylate oxygen (O_8) forms hydrogen bonds with solvent water molecules.

Both inhibitors are further stabilized by additional hydrogen bonds in the active site. For example, the central carboxylate oxygens (O_1 and O_2) of the inhibitor molecules form strong

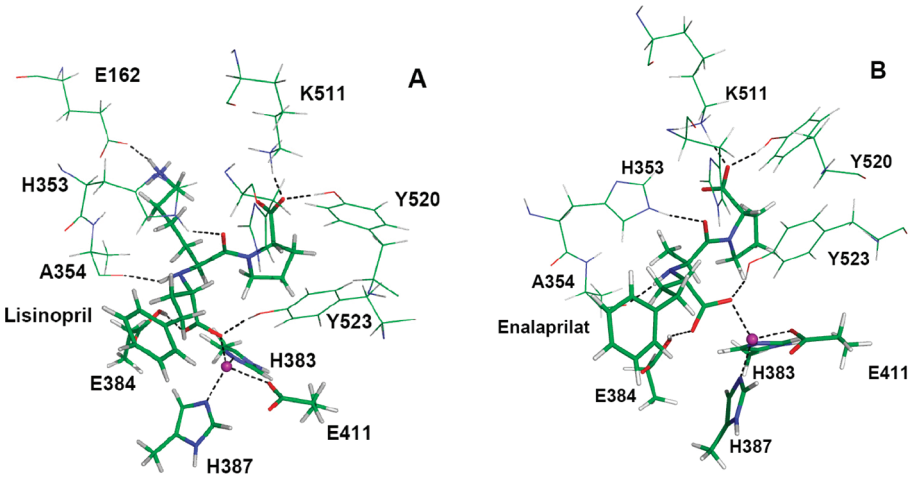

Figure 3. Snapshots of the ACE active site bound to lisinopril (A) and enalaprilat (B), respectively. The zinc ion is color coded purple, and the dash lines are for hydrogen bonds and ligand bonds to the zinc ion.

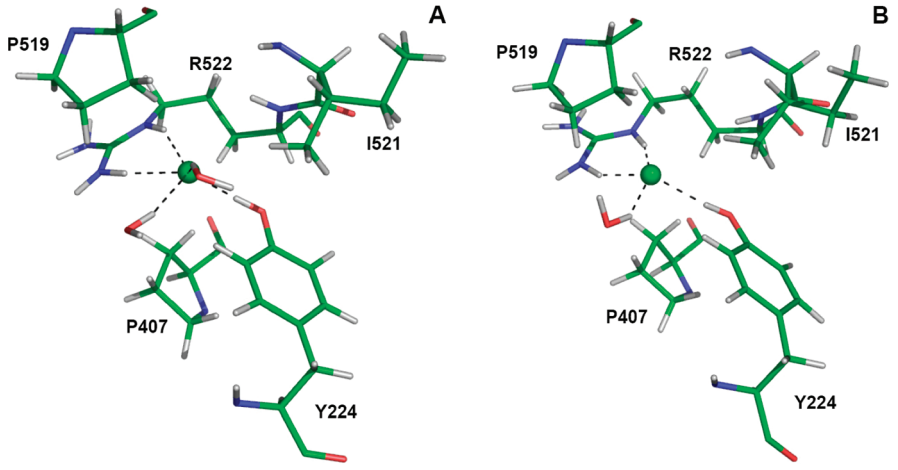

Figure 4. Snapshots for the Cl^-(II) site for the lisinopril-tACE (A) and enalaprilat-tACE (B) complexes. The chloride ion is color coded green, while the dash lines represent the hydrogen bonds to the Cl^- ion.

hydrogen bonds with the Glu384 and Tyr523 side chains. For lisinopril, the $O_2-H_{\varepsilon 2}$(Glu384) and O_1-H_η(Tyr523) distances are 1.82 ± 0.16 Å and 1.72 ± 0.14 Å, respectively. These distances for enalaprilat are 1.78 ± 0.15 Å and 1.86 ± 0.24 Å, respectively. In addition, the backbone amide NH group of the inhibitor forms a hydrogen bond with the backbone carbonyl of Ala354 with a distance of 2.36 ± 0.59 Å for lisinopril and 1.94 ± 0.24 Å for enalaprilat. Furthermore, the backbone carbonyl oxygen (O_7) is hydrogen bonded with His353, evidenced by the $O_7-H_{\varepsilon 2}$(His353) distances of 1.97 ± 0.25 Å for lisinopril and 1.95 ± 0.25 Å for enalaprilat, respectively.

The Cl^-(II) ion has strong electrostatic interactions with side chains of both Arg522 and Tyr224. The distances from H_ε and H_{22} atom of Arg522 to Cl^- are typically less than 2.0 Å, while the distance between H_η atom of Tyr224 and Cl^- is around 1.85 Å for both inhibitors. Additionally, two solvent water molecules are nearby, forming two hydrogen bonds with Cl^-(II). Besides hydrogen bonds from enzyme residues, a hydrophobic shell formed by Pro407, Pro519, and Ile521 may contribute as well. Snapshots of the chloride site for both inhibitor-enzyme complexes are displayed in Figure 4.

3B. Dynamics of Michaelis Complex. The Hip-His-Leu substrate used here to construct the Michaelis complex of ACE has been used by Cushman et al. as a template to design inhibitors to ACE.[23] As shown in Scheme 1, it has a backbone structure similar to those of lisinopril and enalaprilat. As a result, the inhibitor-enzyme complexes discussed above provide a good starting point for constructing the Michaelis complex of ACE. As in the inhibitor-enzyme complexes, the Michaelis complex is quite stable, evidenced by the calculated rmsd of 0.66 ± 0.04 Å for the 1 ns MD simulation. The selected key geometric parameters are listed in Table 4.

Perhaps the most important feature in our model for the Michaelis complex is that the substrate has no direct contact with the zinc ion, in accordance with those observed in the QM/MM simulations of CPA[49] and TLN.[61] In particular, the O_2-Zn distance is 4.51 ± 0.36 Å. Instead, the zinc ion is tetra-coordinated by three protein ligands and a water molecule, which is 2.04 ± 0.06 Å from the zinc ion. The tetra-coordination was kept very well throughout the simulation. In addition to the zinc coordination, this water molecule is also hydrogen bonded strongly with the Glu384 carboxylate group, with an H−O

Table 4. Selected Geometric Parameters of the Michaelis Complex Obtained from the QM/MM MD Simulations Using the SCCDFTB/MM Method

distance (Å) angle (deg)	QM/MM MD
$Zn\cdots O_w$	2.04 ± 0.06
$Zn\cdots O_2$	4.51 ± 0.36
$Zn\cdots N_{\varepsilon 2}$ (H387)	2.01 ± 0.06
$Zn\cdots N_{\varepsilon 2}$ (H383)	2.00 ± 0.05
$Zn\cdots O_{\varepsilon 1}$ (E411)	2.05 ± 0.07
$H_1\cdots O_{\varepsilon 2}$ (E384)	1.34 ± 0.14
$O_2\cdots H_{\varepsilon 2}$ (H513)	2.01 ± 0.36
$O_2\cdots H_{\eta}$(Y523)	1.98 ± 0.25
$C_1\cdots O_w$	3.19 ± 0.26
$O_3\cdots H_{\varepsilon 2}$ (H353)	1.89 ± 0.17
$O_4\cdots H_{\eta}$(Y520)	1.69 ± 0.11
$O_4\cdots H_{\zeta 1}$(K511)	1.71 ± 0.15
$O_5\cdots H_{21}$(Q281)	2.02 ± 0.47
$H_4\cdots$O(A354)	2.02 ± 0.19
Cl···Zn	10.33 ± 0.26
$Cl\cdots H_{\varepsilon}$(R522)	1.94 ± 0.14
$Cl\cdots H_{\eta}$(Y224)	1.83 ± 0.11
$Cl\cdots H_{22}$(R522)	2.00 ± 0.21
$N_{\varepsilon 2}$(H383)···Zn···O_w	100.9 ± 5.4
$N_{\varepsilon 2}$(H387)···Zn···O_w	105.1 ± 6.2
$O_{\varepsilon 1}$(E411)···Zn···O_w	110.1 ± 7.6

distance of 1.34 ± 0.14 Å. Like in CPA and TLN, the Glu384 residue is expected to participate in the catalysis as the general base, which activates the zinc-bound water via proton transfer. Indeed, the putative water nucleophile is ideally located in a near-attack configuration, with a O_w-C_1 distance of 3.19 ± 0.26 Å.

Similar to the lisinopril and enalaprilat inhibitors, the Hip-His-Leu substrate also has a benzene group at the S1 site, which is accommodated by a hydrophobic pocket formed by Phe512 and Val518. In addition, it also has direct contact with some solvent molecules, which suggests that the hydrolysis product can be readily released once the amide bond is cleaved. Similarly, the dimethyl group of the substrate occupies the S2′ site formed by Thr282, Phe457, and Phe527, replacing the proline residue in the inhibitors. However, the S1′ site is not occupied as the imidazole group of the substrate is much shorter than the lysyl group in lisinopril.

The hydrogen-bond network between the substrate and enzyme active site is quite similar to those observed in the inhibitor-enzyme complexes. For example, the C-terminal carboxylate of substrate is stabilized by hydrogen bonds with Tyr520, Lys511, and Gln281, with the $O_4\cdots H_{\eta}$(Tyr520), $O_4\cdots H_{\zeta 1}$(Lys511), and $O_5\cdots H_{21}$(Gln281) distances of 1.69 ± 0.11 Å, 1.71 ± 0.15 Å, and 2.02 ± 0.47 Å, respectively. In addition, the Ala354 backbone oxygen is also hydrogen bonded to a peptide NH group of the substrate with an $O-H_4$ distance of 2.02 ± 0.19 Å. Furthermore, the substrate backbone carbonyl oxygens are hydrogen bonded with His353, His513, and Tyr523, with the hydrogen bond distances of 1.89 ± 0.17 Å for $O_3-H_{\varepsilon 2}$(His353), 2.01 ± 0.36 Å for $O_2-H_{\varepsilon 2}$(His513), and 1.98 ± 0.25 Å for O_2-H_{η}(Tyr523). A snapshot of the active site is displayed in Figure 5.

A similar binding pattern around the Cl^-(II) was found for the Michaelis complex. The chloride ion is tightly held by Tyr224 and Arg522 as well as several solvent water molecules. The distance between Cl^-(II) and zinc ion is 10.33 ± 0.26 Å, which is quite close to that in lisinopril or enalaprilat.

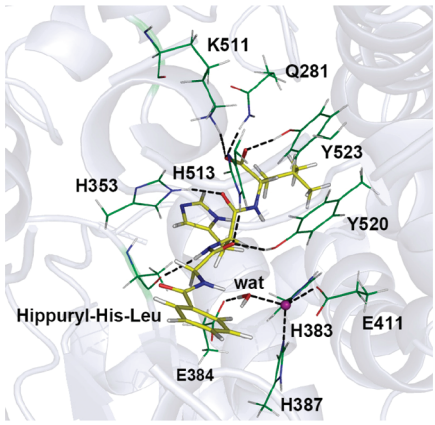

Figure 5. Snapshot for the Michaelis complex of ACE. The Hip-His-Leu substrate is color coded yellow, while the zinc ion is purple.

4. DISCUSSION

ACE has two functional domains, the C and N domains. In this work, QM/MM MD was used to simulate the binding modes of two clinical inhibitors and a natural substrate molecule, Hip-His-Leu, of the testis ACE (tACE), an isoform of the human sACE C-domain. The structure of the substrate-enzyme complex is a prerequisite for a better understanding of the catalysis of ACE. Due to its transient nature, it is very difficult, if not impossible, to obtain structural information of the Michaelis complex. Hence, reliable theoretical models become an important alternative to gain insight into the binding mode and catalysis. In this work, we report a plausible model for the ACE Michaelis complex using a QM/MM simulation method validated by reproducing the structural features of the inhibitor-enzyme complexes observed in X-ray diffraction experiments.

Our model suggests that the substrate in the Michaelis complex is not in direct contact with the zinc ion and the nucleophilic water is the fourth ligand of the metal ion. This model is consistent with the consensus catalytic action of both CPA[62] and TLN,[63] confirmed by recent QM/MM studies.[49,61] Our model assigns the zinc-bound water as the nucleophile and Glu384 as the general base. We further propose that the catalysis is initiated nucleophilic attack at the scissile carbonyl carbon by the nucleophile, assisted by proton transfer to Glu384. The resulting tetrahedral intermediate is stabilized by an oxyanion hole provide by the zinc ion and presumably Tyr523 and His513. The elimination step of the reaction cleaves the C−N bond with the protonation of the leaving group nitrogen by the general acid Glu384. This putative catalytic mechanism has been demonstrated computationally for TLN[61] and CPA,[49] and the resulting barriers are consistent with kinetic data for these two enzymes. Further QM/MM simulations of the catalytic mechanism of ACE will test this mechanism proposal. Work in this direction is underway in our laboratories.

In an earlier publication, Sturrock et al. has proposed a different model for the Michaelis complex of ACE,[7] in which the fourth ligand of the zinc ion is the carbonyl oxygen of the scissile C−N bond, and the water is not zinc bound, but hydrogen bond with the general base (Glu384). This model

was an empirical one, based on the inhibitor-enzyme structures alone. No atomistic interactions were included. Subsequently, a computational model was established for the complex between ACE and the gonadotropin-releasing hormone (GnRH), a natural substrate of ACE.[33] The MD simulations employed the Amber all-atom force field.[64] However, a force field description of the metal−ligand bonds as electrostatic interaction is known to be problematic,[34,35] a bonded model[36] was used for the zinc ion and its ligands, in which the metal−ligand bonds were treated as covalent interactions. As can be expected, such a model has large ambiguities in devising and parametrizing the force field. Indeed, the zinc ion was modeled by Papakyriakou et al.[33] as a penta-coordinated species based on gas phase density functional theory calculations, in which both the nucleophilic water and substrate carbonyl oxygen are zinc ligands. As a result, the MD simulations are restricted to a penta-coordinated zinc configuration. Although penta-coordinated zinc ions are known to exist in enzymes,[65] accurate ab initio QM/MM simulations of TLN[61] has clearly demonstrated that the zinc ion is tetra-coordinated in its active site that is essentially identical to ACE. It may thus be argued that the penta-coordination of the zinc ion in the truncated active-site model of Papakyriakou et al. might be an artifact, attributable to the lack of the enzyme environment. Interestingly, we note that the Amber based classical MD simulations performed by Blumberger et al.[61] on TLN resulted in a stable penta-coordinated zinc cofactor, but the carbonyl oxygen was "expelled from the first coordinate shell" in the first picosecond of the QM/MM simulation.

As discussed above, the two chloride ions play an important role in the binding and catalysis of ACE. Although this study is not aimed at the elucidation of the role of the anions, we would like to comment on some differences between this work and the earlier simulation of the ACE-GnRH complex.[33] In their MD simulations, Papakyriakou et al. found a direct substrate-chloride interaction, thanks to the long peptide substrate (GnRH) used in their simulations, which covers the entire substrate binding crevice of ACE. No such interaction was observed in our simulations, presumably due to the short substrate in our model. Interestingly, we note that some experimental evidence suggested that the absence of Cl^-(II) in the ACE homologue from *Drosophila melanogaster*, AnCE, does not seem to affect the binding of small molecule inhibitors, such as lisnopril and enalaprilat.[16,66] So it is possible that its effect is more pronounced for long chain substrates.

To elucidate the structural role of chloride ions in ACE, it might be desirable to perform longer time MD simulations, with and without the chloride ions. After all, the time scale for protein conformational changes is much longer than that used in the current QM/MM MD simulations.

5. CONCLUSIONS

In this work, we investigated the binding patterns of two well established inhibitors of ACE using a combined QM/MM MD method. The calculated structures using the SCC-DFTB/CHARMM method are in good agreement with those obtained from X-ray diffraction. Based on the inhibitor-enzyme complexes, we propose a plausible model for the Michaelis complex of ACE with the Hip-His-Leu substrate, in which the nucleophilic water is a zinc ligand. QM/MM simulations of this complex yielded useful information that allowed us to propose a catalytic mechanism: The hydrolysis catalyzed by ACE is initiated by the nucleophilic attack of the zinc-bound water at the scissile carbonyl carbon of the substrate, assisted by the Glu384 general base. This is followed by the cleavage of the C−N bond via the elimination of the nitrogen leaving group, again assisted by the Glu384 as the general acid. The binding mode and catalytic mechanism of ACE are thus similar to that of thermolysin and carboxypeptidase A.

AUTHOR INFORMATION

Corresponding Author
*E-mail: dgxu@scu.edu.cn.

ACKNOWLEDGMENT

The authors would thank National Natural Science Foundation of China (Grant No. 20803048 and 21073125) to D. Xu, National Natural Science Foundation of China (Grant No. 20725312 and 91021010) and Chinese Ministry of Science and Technology (2007CB815201) to D. Xie, and National Institutes of Health (R03-AI071992) to H. Guo for the financial support.

REFERENCES

(1) Skeggs, L. T. J.; Kahn, J. R.; Shuway, N. P. The preparation and function of the hypertension-converting enzyme. *J. Exp. Med.* **1956**, *103*, 295–299.

(2) Brown, N. J.; Vaughan, D. E. Angiotensin-converting enzyme inhibitors. *Circulation* **1998**, *97*, 1411–1420.

(3) Zaman, M. A.; Oparil, S.; Calhoun, D. A. Drugs targeting the renin-angiotensin-aldosterone system. *Nat. Rev. Drug Discovery* **2002**, *1*, 621–636.

(4) Ondetti, M. A.; Rubin, B.; Cushman, D. W. Design of specific inhibitors of angiotensin-converting enzyme: new class of orally anti-hypertensive agents. *Science* **1977**, *196*, 441–444.

(5) Patchett, A.; Harris, E.; Tristram, E.; Wyvratt, M.; Wu, M.; Taub, D.; Peterson, E.; Ikeler, T.; Ten Broeke, J.; Payne, L.; Ondeyka, D.; Thorsett, E.; Greenlee, W.; Lohr, N.; Hoffsommer, R.; Joshua, H.; Ruyle, W.; Rothrock, J.; Aster, S.; Maycock, A.; Robinson, F.; Hirschmann, R.; Sweet, C.; Ulm, E.; Gross, D.; Vassil, T.; Stone, C. A new class of angiotensin-converting enzyme inhibitors. *Nature* **1980**, *288*, 280–283.

(6) Natesh, R.; Schwager, S. L. U.; Sturrock, E. D.; Acharya, K. R. Crystal structure of the human angiotensin-converting enzyme-lisinopril complex. *Nature* **2003**, *421*, 551–554.

(7) Sturrock, E. D.; Natesh, R.; van Rooyen, J. M.; Acharya, K. R. Structure of Angiotensin I-Converting Enzyme. *Cell. Mol. Life Sci.* **2004**, *61*, 2677–2686.

(8) Soubrier, F.; Alhenc-Gelas, F.; Huber, C.; Allegrini, J.; John, M.; Tregear, G.; Corvol, P. Two putative active centers in human angiotensin I-converting enzyme revealed by molecular cloning. *Proc. Natl. Acad. Sci. U.S.A.* **1988**, *85*, 9386–9390.

(9) Junot, C.; Gonzales, M. F.; Ezan, E.; Cotton, J.; Vazeux, G.; Michaud, A.; Azizi, M.; Vassiliou, S.; Yiotakis, A.; Corvol, P.; Dive, V. RXP 407, a selective inhibitor of the N-domain of angiotensin I-converting enzyme, blocks in vivo the degradation of hemoregulatory peptide acetyl-Ser-Asp-Lys-Pro with no effect on angiotensin I hydrolysis. *J. Pharmacol. Exp. Ther.* **2001**, *297* (2), 606–611.

(10) Ehlers, M. R. W.; Fox, E. A.; Strydom, D. J.; Riordan, J. F. Molecular cloning of human testicular angiotensin-converting enzyme: the testis isozyme is identical to the C-terminal half of endothelial angiotensin-converting enzyme. *Proc. Natl. Acad. Sci. U.S.A.* **1989**, *86*, 7741–7745.

(11) Natesh, R.; Schwager, S. L. U.; Evans, H. R.; Sturrock, E. D.; Acharya, K. R. Structural Details on the Binding of Antihypertensive

Drugs Captopril and Enalaprilat to Human Testicular Angiotensin I-Converting Enzyme. *Biochemistry* **2004**, *43*, 8718–8724.

(12) Watermeyer, J. M.; Sewell, B. T.; Schwager, S. L.; Natesh, R.; Corradi, H. R.; Acharya, K. R.; Sturrock, E. D. Structure of Testis ACE Glycosylation Mutants and Evidence for Conserved Domain Movement. *Biochemistry* **2006**, *45*, 12654–12663.

(13) Corradi, H. R.; Schwager, S. L. U.; Nchinda, A. T.; Sturrock, E. D.; Acharya, K. R. Crystal structure of the N domain of human somatic angiotensin I-converting enzyme provides a structural basis for domain-specific inhibitor design. *J. Mol. Biol.* **2006**, *357*, 964–974.

(14) Corradi, H. R.; Chitapi, I.; Sewell, T.; Georgiadis, D.; Dive, V.; Sturrock, E. D.; Acharya, K. R. The Structure of Testis Angiotensin-Converting Enzyme in Complex with the C Domain-Specific Inhibitor RXPA380. *Biochemistry* **2007**, *46*, 5473–5478.

(15) Watermeyer, J. M.; Kroger, W. L.; O'Neil, H. G.; Sewell, B. T.; Sturrock, E. D. Probing the Basis of Domain-Dependent Inhibition Using Novel ketone Inhibitors of Angiotensin-Converting Enzyme. *Biochemistry* **2008**, *47*, 5942–5950.

(16) Akif, M.; Georgiadis, D.; mahajan, A.; Dive, V.; Sturrock, E. D.; Isaac, R. E.; Acharya, K. R. High-Resolution Crystal Structures of Drosophila melanogaster Angiotensin-Converting Enzyme in Complex with Novel Inhibitors and Antihypertensive Drugs. *J. Mol. Biol.* **2010**, *400*, 502–517.

(17) Bunning, P.; Riordan, J. F. Activation of angiotensin conveting enzyme by monovalent anions. *Biochemistry* **1983**, *22*, 110–116.

(18) Shapiro, R.; Holmquist, B.; Riordan, J. F. Anion activation of angiotensin converting enzyme: dependence on nature of substrate. *Biochemistry* **1983**, *22*, 3850–3857.

(19) Liu, X.; Fernandez, A.; Wouters, M. A.; Heyberger, S.; Husain, A. Arg(1097) is critical for the chloride dependence of human angiotensin I-converting C-domain catalytic activity. *J. Biol. Chem.* **2001**, *276*, 33518–33525.

(20) Tzakos, A. G.; Galanis, A. S.; Spyroulias, G. A.; Cordopatis, P.; Manessi-Zoupa, E.; Gerothanassis, I. P. Structure-function discrimination of the N- and C- catalytic domains fo human angiotensin-converting enzyme: implications from Cl^- activation and peptide hydrolysis mechanism. *Protein Eng.* **2003**, *16*, 993–1003.

(21) Ondetti, M. A.; Cushman, D. W. *Annu. Rev. Biochem.* **1982**, *51*, 283.

(22) Patchett, A. A.; Cordes, E. H. The design and properties of N-carboxyalkyl-depeptide inhibitors of angiotensin-converting enzyme. *Adv. Enzymol. Relat. Areas Mol. Biol.* **1985**, *57*, 1–84.

(23) Cushman, D. W.; Cheung, H. S.; Sabo, E. F.; Ondetti, M. A. Design of potent competitive inhibitors of angiotensin-converting enzyme. Carboxyalkanoyl and mercaptoalkanoyl amino acids. *Biochemistry* **1977**, *16*, 5484–5491.

(24) Almquist, R. G.; Chao, W. R.; Ellis, M. E.; Johnson, H. L. Synthesis and biological activity of a ketomethylene analog of a tripeptide inhibitor of angiotensin converting enzyme. *J. Med. Chem.* **1980**, *23*, 1392–1398.

(25) Dive, V.; Cotton, J.; Yiotakis, A.; Michaud, A.; Vassiliou, S.; Jiracek, J.; Vazeux, G.; Chauvet, M. T.; Cuniasse, P.; Corvol, P. RXP 407, a phosphinic peptide, is a potent inhibitor of angiotensin I converting enzyme able to differentiate between its two active sites. *Proc. Natl. Acad. Sci. U.S.A.* **1999**, *96*, 4330–4335.

(26) Georgiadis, D.; Beau, F.; Czarny, B.; Cotton, J.; Yiotakis, A.; Dive, V. Roles of the two active sites of somatic angiotensin-converting enzyme in the cleavage of angiotensin I and bradykinin: insights from selective inhibitors. *Circ. Res.* **2003**, *93*, 148–154.

(27) Acharya, K. R.; Sturrock, E. D.; Riordan, J. F. ACE revisited: A new target for structure-based drug design. *Nat. Rev. Drug Discovery* **2003**, *2*, 891–902.

(28) Daull, P.; Jeng, A. Y.; Battistini, B. Towards Triple Vasopeptidase Inhibitors for the Treatment of Cariovascular Diseases. *J. Cardiovasc. Pharmacol.* **2007**, *50* (3), 247–256.

(29) Redelinghuys, P.; Nchinda, A. T.; Sturrock, E. D. Development of Domain-Selective Angiotensin I-Converting Enzyme Inhibitors. *Ann. N. Y. Acad. Sci.* **2005**, *1056*, 160–175.

(30) Sramko, M.; Garaj, V.; Remko, M. Thermodynamics of binding of angiotensin-converting enzyme inhibitors to enzyme active site model. *J. Mol. Struct. (Theochem)* **2008**, *869*, 19–28.

(31) Pina, A. S.; Roque, A. C. A. Studies on the molecular recognition between bioactive peptides and angiotensin-converting enzyme. *J. Mol. Recognit.* **2009**, *22*, 162–168.

(32) Dimitropoulos, N.; Papakyriakou, A.; Dalkas, G. A.; Sturrock, E. D.; Spyroulias, G. A. A Computational Approach to the Study of the Binding Mode of Dual ACE/NEP Inhibitors. *J. Chem. Inf. Model.* **2010**, *50*, 388–396.

(33) Papakyriakou, A.; Spyroulias, G. A.; Sturrock, E. D.; Manessi-Zoupa, E.; Cordopatis, P. Simulated Interactions between Angiotensin-Converting Enzyme and Substrate Gonadotropin-Releasing Hormone: Novel Insights into Domain Selectivity. *Biochemistry* **2007**, *46*, 8753–8765.

(34) Li, X.; Hayik, S. A.; Merz, K. M., Jr. QM/MM X-ray refinement of zinc metalloenzymes. *J. Inorg. Biochem.* **2010**, *104*, 512–522.

(35) Wu, R.; Hu, P.; Wang, S.; Cao, Z.; Zhang, Y., Flexibility of catalytic zinc coordination in thermolysin and HDAC8: A Born-Oppenheimer ab initio QM/MM molecular dynamics study. *J. Chem. Theory Comput.* **in press**.

(36) Hoops, S. C.; Anderson, K. W.; Merz, J., K. M. Force-field design for metalloproteins. *J. Am. Chem. Soc.* **1991**, *113*, 8262–8270.

(37) Warshel, A.; Levitt, M. Theoretical studies of enzymatic reactions: Dielectric, electrostatic and steric stabilization of carbonium ion in the reaction of lysozyme. *J. Mol. Biol.* **1976**, *103*, 227–249.

(38) Field, M. J.; Bash, P. A.; Karplus, M. A combined quantum mechanical and molecular mechanical potential for molecular dynamics simulations. *J. Comput. Chem.* **1990**, *11*, 700–733.

(39) Gao, J., Methods and applications of combined quantum mechanical and molecular mechanical potentials. In *Rev. Comput. Chem.*, Lipkowitz, K. B.; Boyd, D. B., Eds.; VCH: New York, 1996; Vol. 7, pp 119−185.

(40) MacKerell, A. D., Jr.; Bashford, D.; Bellott, M.; Dunbrack, R. L., Jr.; Evanseck, J. D.; Field, M. J.; Fischer, S.; Gao, J.; Guo, H.; Ha, S.; Joseph-McCarthy, D.; Kuchnir, L.; Kuczera, K.; Lau, F. T. K.; Mattos, C.; Michnick, S.; Ngo, T.; Nguyen, D. T.; Prodhom, B.; Reiher, W. E., III; Roux, B.; Schlenkrich, M.; Smith, J. C.; Stote, R.; Straub, J.; Watanabe, M.; Wiorkiewicz-Kuczera, J.; Yin, D.; Karplus, M. All-atom empirical potential for molecular modeling and dynamics studies of proteins. *J. Phys. Chem. B* **1998**, *102*, 3586–3616.

(41) Jorgensen, W. L.; Chandrasekhar, J.; Madura, J. D.; Impey, R. W.; Klein, M. L. Comparison of simple potential functions for simulating liquid water. *J. Chem. Phys.* **1983**, *79*, 926–935.

(42) Elstner, M.; Frauenheim, T.; Kaxiras, E.; Seifert, G.; Suhai, S. A self-consistent charge density-functional based tight-binding scheme for large biomolecules. *Phys. Status Solidi* **2000**, *B217*, 357–376.

(43) Cui, Q.; Elstner, M.; Kaxiras, E.; Frauenheim, T.; Karplus, M. A QM/MM implementation of the self consistent charge density functional tight binding (SCC-DFTB) method. *J. Phys. Chem. B* **2001**, *105*, 569–585.

(44) Riccardi, D.; Schaefer, P.; Yang, Y.; Yu, H.; Ghosh, N.; Prat-Resina, X.; Konig, P.; Li, G.; Xu, D.; Guo, H.; Elstner, M.; Cui, Q. Development of effective quantum mechanical/molecular mechanical (QM/MM) methods for complex biological processes. *J. Phys. Chem. B* **2006**, *110*, 6458–6469.

(45) Elstner, M.; Cui, Q.; Munih, P.; Kaxiras, E.; Frauenheim, T.; Karplus, M. Modeling zinc in biomolecules with the self consistent charge density functional tight binding (SCC-DFTB) method: Applications to structure and energetic analysis. *J. Comput. Chem.* **2003**, *24*, 565–581.

(46) Riccardi, D.; Cui, Q. pKa analysis for the zinc-bound water in human carbonic anhydrase II: benchmark for "multi-scale" QM/MM simulations and mechanistic implications. *J. Phys. Chem. A* **2007**, *111*, 5703–5711.

(47) Riccardi, D.; Konig, P.; Guo, H.; Cui, Q. Proton transfer in carbonic anhydrase is controlled by electrostatics rather than the orientation of the acceptor. *Biochemistry* **2008**, *47*, 2369–2378.

(48) Xu, D.; Guo, H. Quantum mechanical/molecular mechanical and density functional theory studies of a prototypical zinc peptidase (carboxypeptidase A) suggest a general acid-general base mechanism. *J. Am. Chem. Soc.* **2009**, *131*, 9780–9788.
(49) Wu, S. S.; Zhang, C. C.; Xu, D. G.; Guo, H. Catalysis of Carboxypeptidase A: Promoted-Water versus Nucleophilic Pathways. *J. Phys. Chem. B* **2010**, *114* (28), 9259–9267.
(50) Xu, D.; Zhou, Y.; Xie, D.; Guo, H. Antibiotic binding to monozinc CphA β-lactamase from Aeromonas hydropila: quantum mechanical/molecular mechanical and density functional theory studies. *J. Med. Chem.* **2005**, *48*, 6679–6689.
(51) Xu, D.; Xie, D.; Guo, H. Catalytic mechanism of class B2 metallo-β-lactamase. *J. Biol. Chem.* **2006**, *281*, 8740–8747.
(52) Wang, C.; Guo, H. Inhibitor binding by metallo-β-lactamase IMP-1 from Pseudomonas aeruginosa: Quantum mechanical/molecular mechanical simulations. *J. Phys. Chem. B* **2007**, *111*, 9986–9992.
(53) Xu, D.; Guo, H.; Cui, Q. Antibiotic deactivation by dizinc β-lactamase: mechanistic insights from QM/MM and DFT studies. *J. Am. Chem. Soc.* **2007**, *129*, 10814.
(54) Xu, D.; Guo, H.; Cui, Q. Antibiotic binding to dizinc β-lactamase L1 from Stenotrophomonas maltophilia: SCC-DFTB/CHARMM and DFT studies. *J. Phys. Chem. A* **2007**, *111*, 5630–5636.
(55) Wu, S.; Xu, D.; Guo, H. QM/MM studies of mono-zinc beta-lactamase CphA suggest that the crystal structure of an enzyme-intermediate complex represents a minor pathway. *J. Am. Chem. Soc.* **2010**, *132*, 17986–17988.
(56) Brooks, C. L., III; Karplus, M. Solvent effects on protein motion and protein effects on solvent motion. *J. Mol. Biol.* **1989**, *208*, 159–181.
(57) Steinbach, P. J.; Brooks, B. R. New spherical-cutoff methods for long-range forces in macromolecular simulations. *J. Comput. Chem.* **1994**, *15*, 667.
(58) Ryckaert, J. P.; Ciccotti, G.; Berendsen, H. J. Numerical integration of the cartesian equations of motion of a system with constraints: molecular dynamics of n-alkanes. *J. Comput. Phys.* **1977**, *23*, 327–341.
(59) Vrielink, A.; Obel-Jorgensen, A.; Codding, P. W. Hippuryl-L-histidyl-L-leucine, a Substrate for Angiotensin Converting Enzyme. *Acta Crystallogr., Sect. C: Cryst. Struct. Commun.* **1996**, *C52*, 1300–1302.
(60) Hangauer, D. G.; Mozingo, A. F.; Matthews, B. W. An interactive computer graphics study of thermolysin-catalyzed peptide cleavage and inhibition by N-carboxymethyl dipeptides. *Biochemistry* **1984**, *23*, 5730–5741.
(61) Blumberger, J.; Lamoureux, G.; Klein, M. L. Peptide hydrolysis in thermolysin: Ab initio QM/MM investigation of the Glu143-assisted water addition mechanism. *J. Chem. Theory Comput.* **2007**, *3*, 1837–1850.
(62) Christianson, D. W.; Lipscomb, W. N.; Carboxypeptidase, A. *Acc. Chem. Res.* **1989**, *22*, 62–69.
(63) Matthews, B. W. Structural basis of the action of thermolysin and related zinc peptidases. *Acc. Chem. Res.* **1988**, *21*, 333–340.
(64) Cornell, W. D.; Cieplak, P.; Bayly, C. I.; Gould, I. R.; Merz, J., K. M.; Ferguson, D. M.; Spellmeyer, D. C.; Fox, T.; Caldwell, J. W.; Kollman, P. A. A second generation force field for the simulation of protein, nucleic acids, and organic molecules. *J. Am. Chem. Soc.* **1995**, *117*, 5179.
(65) Lipscomb, W. M.; Strater, N. Recent advances in zinc enzymology. *Chem. Rev.* **1996**, *96*, 2375–2433.
(66) Kim, H. M.; Shin, D. R.; Yoo, O. J.; Lee, H.; Lee, J. O. Crystal structure of Drosophila angiotensin I-converting enzyme bound to captopril and lisinopril. *FEBS Lett.* **2003**, *538*, 65–70.